Journal of Computer and Communications, 2023, 11, 70-83
https://www.scirp.org/journal/jcc
ISSN Online: 2327-5227
ISSN Print: 2327-5219

Research on Electromagnetic Acoustic Emission Signal Recognition Based on Local Mean Decomposition and Least Squares Support Vector Machine

Chenglong Yang[1], Yushu Lai[2*], Qiuyue Li[1]

[1]School of Electronic and Information Engineering, Chongqing Three Gorges University, Chongqing, China
[2]Chongqing Engineering Technology Research Center for Light Alloy and Processing, Chongqing, China
Email: *yangclyy@yeah.net

How to cite this paper: Yang, C.L., Lai, Y.S. and Li, Q.Y. (2023) Research on Electromagnetic Acoustic Emission Signal Recognition Based on Local Mean Decomposition and Least Squares Support Vector Machine. *Journal of Computer and Communications*, **11**, 70-83.
https://doi.org/10.4236/jcc.2023.115006

Received: April 26, 2023
Accepted: May 26, 2023
Published: May 29, 2023

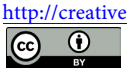

Abstract

Electromagnetic acoustic emission technology is one of nondestructive testing, which can be used for defect detection of metal specimens. In this study, round and cracked metal specimens, round metal specimens, and intact metal specimens were prepared. And the electromagnetic acoustic emission signals of the three specimens were collected. In addition, the local mean decomposition(LMD), Autoregressive model(AR model) and least squares support vector machine (LSSVM) algorithms were combined to identify the eletromagnetic acoustic emission signals of round and cracked, round, and intact specimens. According to the algorithm recognition results, the recognition accuracy of can reach above 97.5%, which has a higher recognition rate compared with SVM and BP neural network. The results of the study show that the algorithm is able to identify quickly and accurately crack defect in metal specimens.

Keywords

Electromagnetic Acoustic Emission Technology, LMD, LSSVM, Defect Detection of Metal Crack

1. Introduction

High-performance metals and their alloys are widely used in aerospace, petroleum and petrochemical, machinery manufacturing, transportation and other industrial fields [1] [2]. And metals and their alloys are used under pressure and force for a long time, leading to micro-cracks on the metal surface. If cracks are

not detected in time, the cracks will extend during the use of metal structural parts, leading to fracture, causing casualties and property damage, and triggering serious safety accidents [3]. At present, the conventional nondestructive testing methods for metal crack defects mainly include: Ultrasonic Testing [4], Radiographic Testing [5], Magnetic Flux Leakage [6], Eddy Current Testing [7], Penetration Testing [8] and Acoustic Emission [9]. Each technology has corresponding application areas and different defect detection capabilities, but all have certain limitations, such as Ultrasonic Testing and Radiographic Testing for the detection of defects within the metal structure, Magnetic Flux Leakage, Eddy Current Testing and Penetration Testing for the detection of surface and near-surface cracks in metal specimens. Compared with other NDT methods, Acoustic Emission can receive acoustic emission signals in real time, which is easy to realize online detection; it can detect dynamic cracks, crack sprouting and crack growth of metal structural parts. However, there are also problems such as harsh loading conditions, poor repeatability and noise interference. Therefore, on the basis of the existing NDT methods, the improvement and development of new inspection techniques and the integration and application of various NDT will become the main development trend in the field of NDT [10]. Electromagnetic acoustic emission technology combines electromagnetic detection technology and acoustic emission detection technology, which has well detection capability for small cracks. The basic principle is to load an electric current through a coil on top of a metal specimen with defects (such as cracks, pores or inclusions), and the current concentration effect occurs at the defective area to form a high density current, which generates Lorentz force at the defective area of the metal specimen and thus excites the acoustic emission signal [11] [12] [13]. Thus, this technology enables the detection of cracks in sheet metal specimens and tubular metal specimens.

2. Literature Review

Currently, the focus of research on the electromagnetic acoustic emission technology has shifted to signal processing. The main signal processing methods are FFT, wavelet packet transform, Hilbert-Yellow transform [14], etc, which analyze electromagnetic acoustic emission signals from different perspectives. In the literature, a combination of wavelet packet transform and energy entropy was used to achieve electromagnetic acoustic emission signal feature extraction and input to BP neural network for identification, and a high accuracy rate was obtained [15].

Local mean decomposition is an adaptive signal decomposition method that can decompose a signal into several PF components and is suitable for the processing of non-stationary nonlinear signals [16] [17]. The upper and lower envelopes obtained by the LMD decomposition using the smoothing algorithm can effectively solve the under-envelope problem and the endpoint effect in the EMD decomposition. AR model is a time series model, and the autoregressive

parameters of the model are sensitive to changes in status and can be used as feature vectors for acoustic emission signal identification [18] [19]. LSSVM is an improved SVM with stronger generalization ability, which has better advantages in small sample classification recognition [20] [21]. Based on the above research results, the paper uses the LMD algorithm to decompose the electromagnetic acoustic emission signal to obtain the PF component signal, and selects the optimal PF component signal according to the energy occupation ratio method. The AR model of the component signal is built, and the optimal order of the model is determined by the AIC criterion. The autoregressive parameters and mean square deviation of the AR model are extracted as feature vectors, which is fed into the LSSVM classifier for signal recognition.

3. Methodology

3.1. Local Mean Decomposition

Local mean decomposition is an adaptive signal decomposition method that can decompose a complex non-smooth signal into a finite number of smooth single component signals and a monotonic function adaptively, which is applicable to the processing of non-stationary and non-linear signals. The specific steps are as follows [16]:

Find all local extrema n_i from the original signal $x(t)$ and the average function m_i and envelope estimation function a_i of two adjacent extrema n_i and n_{i+1} can be calculated by

$$\begin{cases} m_i = \dfrac{n_i + n_{i+1}}{2} \\ a_i = \dfrac{|n_i - n_{i+1}|}{2} \end{cases} \tag{1}$$

The local mean function $m_{11}(t)$ is obtained by connecting all the mean functions with straight lines and smoothing them by sliding translation method. The local envelope estimation function $a_{11}(t)$ is obtained by connecting all the envelope estimates with a straight line and smoothing them by the sliding translation method.

The local mean function $m_{11}(t)$ is subtracted from the original signal $x(t)$ and the resulting signal $h_{11}(t)$ is given by

$$h_{11}(t) = x(t) - m_{11}(t) \tag{2}$$

The FM signals $s_{11}(t)$ can be obtained by dividing $h_{11}(t)$ by $a_{11}(t)$.

$$s_{11}(t) = \frac{h_{11}(t)}{a_{11}(t)} \tag{3}$$

The ideal FM signals $s_{11}(t)$ is a pure FM function. In other words, envelope estimation function $a_{12}(t) \approx 1$. If $s_{11}(t)$ is not a pure FM function, then $s_{11}(t)$ is regarded as the original signal to calculate repetitively above procedure until $s_{11}(t)$ becomes a pure FM function.

The envelope signal $a_1(t)$ can be obtained by multiplying the envelope estimation functions of the above iterations.

$$a_1(t) = a_{11}(t)a_{12}(t)\cdots a_{1n}(t) = \prod_{q=1}^{n} a_{1q}(t) \tag{4}$$

The first PF component signal of the original signal can be obtained by multiplying the envelope signal $a_1(t)$ and the pure FM signal $s_{1n}(t)$.

$$PF_1(t) = a_1(t)s_{1n}(t) \tag{5}$$

$u_1(t)$ can be obtained by separating the component signals $PF_1(t)$ from the original signal $x(t)$. $u_1(t)$ can be considered as a new original signal and the above process is repeated. After *k* cycles, until *k* becomes a monotonic function.

$$\begin{cases} u_1(t) = x(t) - PF_1(t) \\ u_2(t) = u_1(t) - PF_2(t) \\ \quad\vdots \\ u_k(t) = u_{k-1}(t) - PF_k(t) \end{cases} \tag{6}$$

Thus, the original signal $x(t)$ can be decomposed into a sum of k-PF components and a monotonic function $u_k(t)$.

$$x(t) = \sum_{p=1}^{k} PF_p(t) + u_k(t) \tag{7}$$

3.2. AR Model

AR model is a type of time series model, and its autoregressive parameters are sensitive to changes in the underlying patterns, making it suitable as a feature vector for acoustic emission signal recognition.

3.2.1. AR Model Principle

The following AR model can be established for a stationary time series $\{x_k\}(k = 1, 2, \cdots, N)$:

$$x_k = \phi_1 x_{k-1} + \phi_2 x_{k-2} + \cdots + \phi_m x_{k-m} + a_k = \sum_{i=1}^{m} \phi_i x_{k-i} + a_k \tag{8}$$

where, $\phi_i(i = 1, 2, \cdots, m)$ is the autoregressive coefficient, m is the order of the model, and $\{a_k\}(k = 1, 2, \cdots)$ is a set of uncorrelated discrete white noise sequences with mean 0 and variance $\delta_a^2\left(0 < \delta_a^2 < \infty\right)$.

The key to establishing an AR model is to solve the model parameters and determine the model order, as can be seen from Equation (8). The autoregressive parameters of AR model can be determined using the method of least squares, which has the advantage of being computationally simple and fast. The optimal model order can be determined using the Akaike information criterion (AIC), which can improve the accuracy of building the model. Thus, in this paper, the model parameters are calculated using the least squares method, and the model order is determined based using the AIC criterion.

3.2.2. Least Squares Estimation of AR Model Parameters

The specific steps for using the least squares method to solve the AR model coefficients $\phi_i\left(i=1,2,\cdots,m\right)$ and mean squared error are as follows [19]:

From equation (8), the model order can be obtained by

$$a_k = x_k - \phi_1 x_{k-1} - \phi_2 x_{k-2} - \cdots - \phi_m x_{k-m} \tag{9}$$

For the AR model, δ_a^2 is the mean square error of the model residual sequence. Therefore

$$\delta_a^2 = E\left(a_k^2\right) = \frac{1}{N}\sum_{k=m+1}^{N} E\left(x_k - \phi_1 x_{k-1} - \phi_2 x_{k-2} - \cdots - \phi_m x_{k-m}\right) \tag{10}$$

The coefficients are determined according to the principle of least squares, even if the mean square deviation reaches its minimum. Then, this is transformed into the problem of finding the extremum of a multivariate function. Therefore

$$\begin{cases} \dfrac{\partial\delta}{\partial\phi_1} = E\left[2\left(x_k - \phi_1 x_{k-1} - \phi_2 x_{k-2} - \cdots - \phi_m x_{k-m}\right)\left(-x_{k-1}\right)\right] = 0 \\ \dfrac{\partial\delta}{\partial\phi_2} = E\left[2\left(x_k - \phi_1 x_{k-1} - \phi_2 x_{k-2} - \cdots - \phi_m x_{k-m}\right)\left(-x_{k-2}\right)\right] = 0 \\ \vdots \\ \dfrac{\partial\delta}{\partial\phi_m} = E\left[2\left(x_k - \phi_1 x_{k-1} - \phi_2 x_{k-2} - \cdots - \phi_m x_{k-m}\right)\left(-x_{k-m}\right)\right] = 0 \end{cases} \tag{11}$$

After simplification and consolidation, it can be expressed in matrix form

$$P_m \varphi = \rho \tag{12}$$

where, $P_m = \begin{bmatrix} 1 & \rho_1 & \rho_2 & \cdots & \rho_{m-1} \\ \rho_1 & 1 & \rho_1 & \cdots & \rho_{m-2} \\ \vdots & \vdots & \vdots & \ddots & \vdots \\ \rho_{m-1} & \rho_{m-2} & \rho_{m-3} & \cdots & 1 \end{bmatrix}$, $\varphi = \left[\phi_1, \phi_2, \cdots, \phi_m\right]^{\mathrm{T}}$, $\rho = \left[\rho_1, \rho_2, \cdots, \rho_m\right]^{\mathrm{T}}$.

Equation (12) is called the Yule-Walker equation, where P_m is the autocorrelation matrix that belongs to the Toeplitz matrix, φ is the parameter matrix, and ρ is the autocorrelation coefficient matrix. The autocorrelation coefficients $\rho_i\left(i=1,2,\cdots,m\right)$ can be calculated by $\left\{x_k\right\}\left(k=1,2,\cdots,N\right)$, and the parameter matrix φ can be obtained by solving a linear system of equations. Therefore

$$\varphi = P_m^{-1}\rho \tag{13}$$

During the inversion of the autocorrelation matrix, the Levinson recursive algorithm can be used.

3.2.3. Minimum Information Criterion-AIC Guideline

The principle of Minimum Information Criterion is to prefer the model with the lowest AIC value when selecting the best model from a set of models [22]. The formula is that

$$\mathrm{AIC}(m) = \ln\left(\delta_a^2\right) + \frac{2m}{N} \tag{14}$$

where, N the data length, δ_a^2 is the mean squared error of the model, and m is the order of the model.

4. Electromagnetic Acoustic Emission Signal Feature Extraction

A total of three types of metal specimens were prepared as research objects, including specimens with circular holes and cracks, specimens with only circular holes, and intact specimens, for conducting electromagnetic acoustic emission experiments. The signals collected through the experiment are non-stationary and non-linear, and signal characteristics cannot be accurately reflected by using conventional signal processing methods. Therefore, the LMD decomposition was applied to the electromagnetic acoustic emission signal to convert the complex non-stationary signals into stationary signals. The optimal PF component signal was selected to establish an AR model, and the autoregressive parameters and mean square deviation of the model were extracted as characteristic vectors. The feature extraction process of electromagnetic acoustic emission is shown in Figure 1.

4.1. Experiment of Electromagnetic Acoustic Emission

The electromagnetic excitation was performed using a Model-10030 programmable current source and a CH-130 electromagnet, while the signal was acquired using an SAEU2S digital acoustic emission transmitter, as shown in Figure 2. The SR150N sensor was used arranged at 10 cm from the crack defect using a coupling agent to ensure the integrity of the acquired signals, as shown in Figure 3. The electromagnetic excitation method is 0 A gradually loaded to 20 A and then 20 A down to 0 A.

Magnesium alloy is widely used in industrial fields such as aerospace and transportation. Therefore, this paper selects magnesium alloy AZ31B as the research object. Three thin plate specimens were prepared, respectively: 1# magnesium alloy specimen with a pre-fabricated circular hole and crack in the center, simulating crack defects around bolt holes of large metal components in industry; 2# magnesium alloy specimen with a pre-fabricated circular hole in the center, simulating screw holes in large metal components in industry; 3# magnesium alloy specimen without any pre-fabricated holes or cracks in the center. The geometry of the magnesium alloy specimen is 300 mm × 100 mm × 1 mm, the radius of the circular hole is 5 mm, and the crack size is 15 mm × 1 mm.

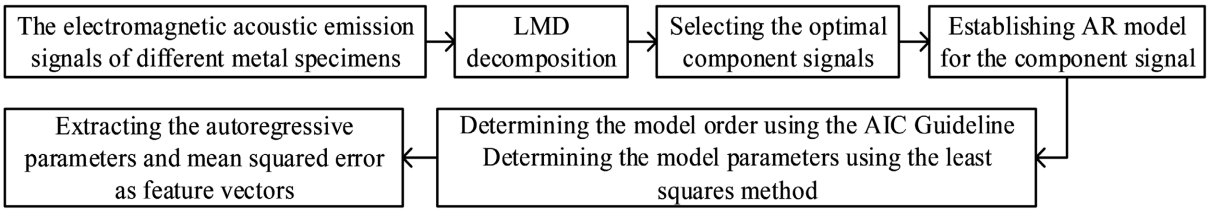

Figure 1. Flow chart of feature extraction.

After multiple repeated experiments, the experimental results are shown in Figure 4.

Figure 2. Example of a figure caption (figure caption).

Figure 3. Arrangement diagram of sensor.

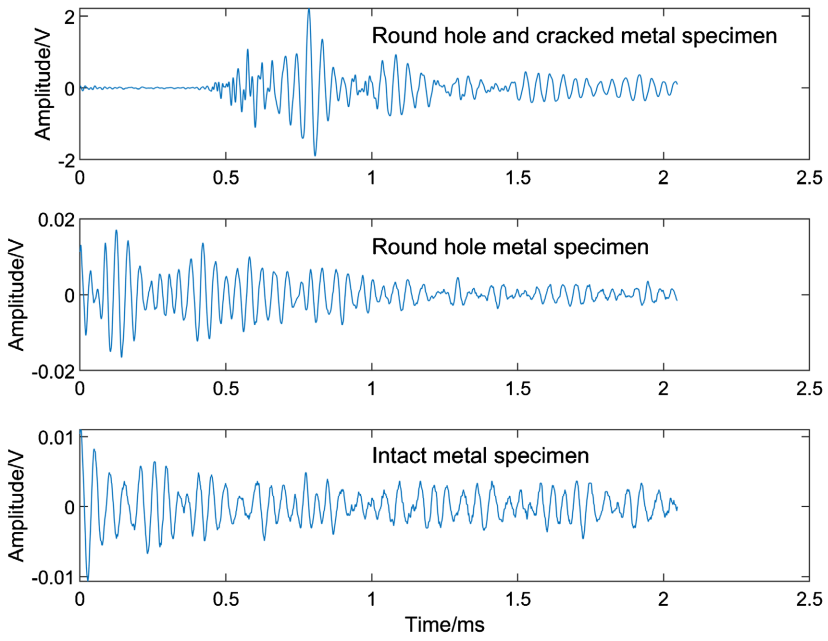

Figure 4. Original signal of electromagnetic acoustic emission.

4.2. LMD Decomposition and Building AR Model

The experimentally acquired electromagnetic acoustic emission signals were subjected to LMD decomposition, and the decomposition results are shown in Figure 5.

In order to select the optimal PF component signals from the LMD component signals for analysis, the energy percentage of each PF component was calculated, and the results are shown in Table 1. From Table 1, we can see that the PF_1 component signal energy accounts for the most percentage of the original signal energy, indicating that it contains more information of the original signal, so PF_1 is chosen for the study.

AR models were separately established for the component signals of the three specimen signals, and the variation of the value of the criterion function AIC with the order of the model was plotted as shown in Figure 6.

As can be seen from Figure 6, when the model order $m > 5$, the variation of

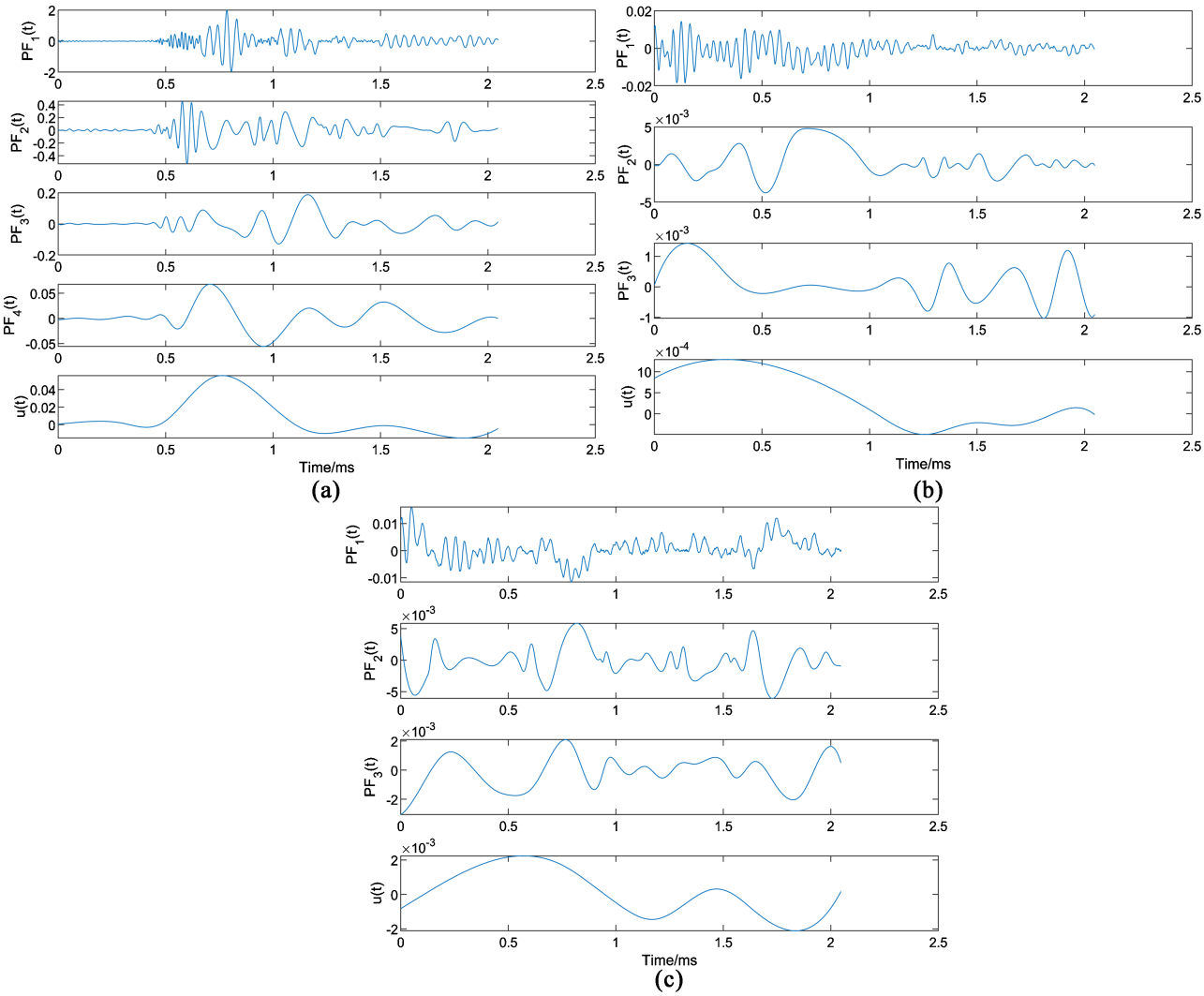

Figure 5. PF component of electromagnetic acoustic emission signal. (a) PF component of the round hole and cracked metal specimen; (b) PF component of the round hole metal specimen; (c) PF component of the intact metal specimen.

Table 1. The energy percentage of each PF component.

Energy Percentage	PF_1	PF_2	PF_3	PF_4	u_k
The round hole and cracked specimen	89.05%	8.52%	1.78%	0.38%	0.28%
The round hole specimen	83.28%	13.62%	1.21%		1.88%
The intact specimen	65.76%	22.72%	4.68%		6.84%

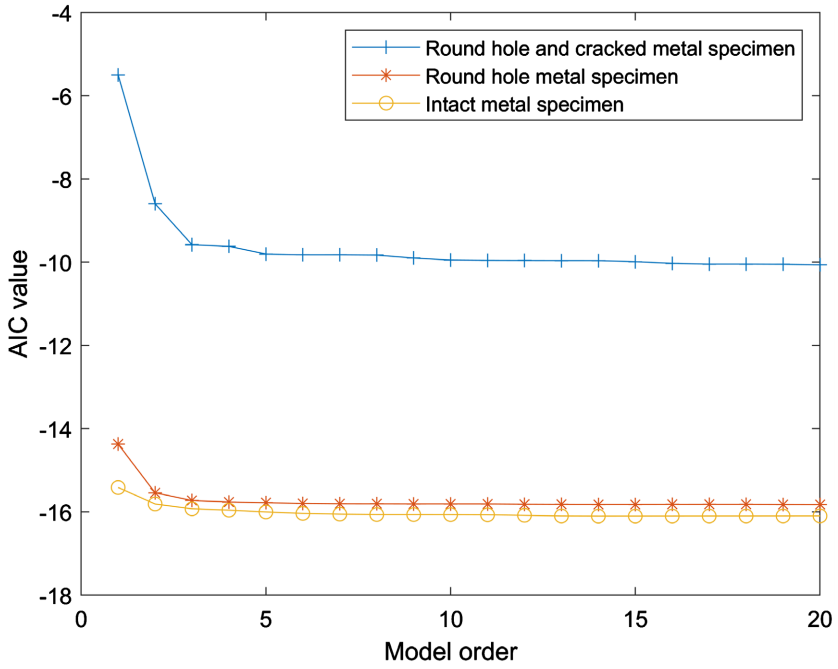

Figure 6. Variation of AIC value with model order.

AIC values are small and less than AIC values of 1 to 5. Therefore, the optimal order of the AR model can be determined as 5. The first 5 autoregressive parameters and mean squared error of the AR model for each dataset are extracted as feature vectors.

4.3. Feature Extraction

Based on the above method, the electromagnetic acoustic emission signals of the three specimens were decomposed by using LMD algorithm, and an AR model was established for the optimal PF component signals. And the first 5th order autoregressive parameters $\varphi_k\left(k=1,2,\cdots,5\right)$ and mean square deviation δ_a^2 of the AR models were extracted to form a six-dimensional feature vector. Some of the AR parameters are shown in Table 2.

By observing Table 2, it can be found that the numerical changes of the autoregressive parameters and mean square deviation characteristics of the same type of metal specimens have limited and relatively stable variations. The ranges of the autoregressive parameters and mean squared error features for different types of metal specimens are slightly different. Among them, the absolute values of the autoregressive parameters of the round hole and crack metal specimens

Table 2. Partial AR parameters.

Metal specimen	φ_1	φ_2	φ_3	φ_4	φ_5	δ_a^2
Round hole and cracked	−2.9418	2.8767	−0.4928	−0.8290	0.3951	3.89E−05
Round hole and cracked	−2.0383	1.3508	−0.0319	−0.4762	0.2343	2.72E−07
Round hole and cracked	−1.9170	1.0715	0.1635	−0.5093	0.2281	2.38E−07
Round hole and cracked	−2.2122	1.1412	0.3830	−0.2648	−0.0401	1.38E−06
Round hole and cracked	−2.6136	2.4251	−0.6436	−0.3884	0.2402	8.01E−05
Round hole metal specimen	−1.4429	0.1728	0.2142	0.0290	0.0629	1.37E−07
Round hole metal specimen	−1.3133	0.0867	0.0792	0.0313	0.1608	8.72E−07
Round hole metal specimen	−1.3550	0.1593	0.1557	−0.0284	0.0964	1.44E−07
Round hole metal specimen	−1.6210	0.4306	0.2637	−0.1459	0.0944	1.07E−07
Round hole metal specimen	−1.5854	0.2668	0.2323	0.2035	−0.0879	2.42E−06
Intact metal specimen	−1.3174	0.1161	0.1270	−0.0600	0.1500	1.20E−07
Intact metal specimen	−1.2278	−0.1280	0.1618	0.1262	0.1037	2.86E−06
Intact metal specimen	−1.3324	0.1209	0.1216	−0.0315	0.1475	1.56E−07
Intact metal specimen	−1.4085	0.1436	0.1701	0.0361	0.0794	2.06E−07
Intact metal specimen	−1.2386	0.0663	0.0696	−0.0259	0.1534	1.85E−07

are relatively large compared to other metal specimens. Therefore, it is feasible and effective to extract electromagnetic acoustic emission signal features by using LMD and AR modeling methods.

5. Research Results

5.1. LSSVM Identification

The round hole metal specimens with crack defects were considered as one category, and a total of 40 sets of experimental data were collected, which category label is 1. The round hole metal specimens and intact metal specimens without crack defects were considered as one category, and 20 sets of experimental data were collected separately, for a total of 40 sets of experimental data, which category label is 2. Randomly select 20 sets of data from each category as training samples, and the remaining 20 sets as test samples. That is, 40 sets of data are used for training and 40 sets of data are used for testing.

The feature vectors are input into LSSVM for training and testing, and the regularization parameters and kernel function parameters are optimized by using 5-fold cross-validation. The optimization result of the regularization parameter is $\gamma = 3.6816$, the optimization result of the kernel function parameter is $\sigma^2 = 1.8455$, and the identification result is shown in **Figure 7**.

From **Figure 7**, it can be seen that in the recognition of electromagnetic acoustic emission signals by LSSVM, there is only one misclassification in the 40 test samples, and the recognition accuracy of the test set can reach 97.5%. The

identification of the circular hole and crack metal specimens is all correct, while there is one error in the identification of normal metal specimens, indicating that the LSSVM classifier can accurately distinguish metal specimens with crack defects from normal metal specimens.

5.2. Algorithm Comparison and Analysis

The LSSVM was compared with the BP neural network and SVM, and the comparison results are shown in Table 3. It can be seen that the LSSVM is superior to both the BP neural network and SVM in terms of recognition accuracy and training time.

The combination of LMD and AR model for electromagnetic acoustic emission feature extraction is proved to be very effective through experiments. It is also proved that LSSVM can effectively solve the small sample and nonlinear classification problems, and it is proved that the combination of LMD and LSSVM can be effectively used in electromagnetic acoustic emission signal classification and recognition, which is a new method for electromagnetic acoustic emission signal classification and recognition, and can realize the detection of

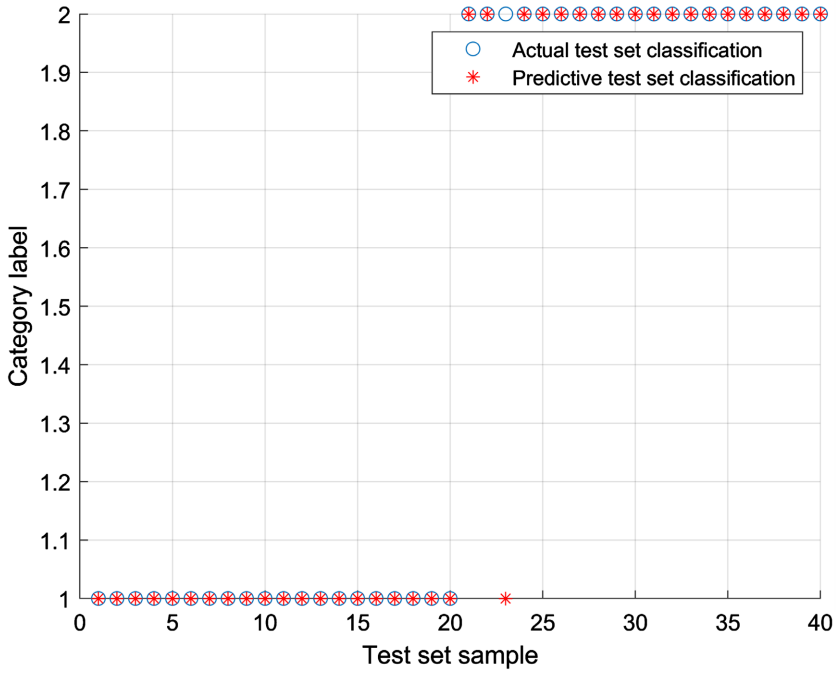

Figure 7. Identification result chart.

Table 3. Comparison of identification results.

Classifier	Training Sample	Test Sample	Correct identification number	Recognition accuracy	Training time
LSSVM	40	40	39	97.5%	0.21s
SVM	40	40	36	90%	1.26s
BPNN	40	40	34	85%	0.37s

metal cracks.

6. Conclusions and Implication

A method combining LMD, AR model, and LSSVM is proposed to recognize the electromagnetic acoustic emission signals, addressing the challenge of extracting features from non-stationary signals. Firstly, the LMD algorithm is used to transform the electromagnetic acoustic emission signals into stationary component signals. Then, the best component signal is selected from the component signal by the energy occupation method and an AR model is established. And the autoregressive parameters and mean squared error extracted from the model are used to construct a six-dimensional feature vector. Finally, the feature vectors were trained and tested using LSSVM, SVM, and BP neural networks. in which the test set recognition accuracy of LSSVM can reach 97.5%, the test set recognition accuracy of SVM is 90%, and the test set recognition accuracy of BP neural network is 85%. It is proved through experiments that the combination of LMD, AR model and LSSVM has high superiority in the identification of electromagnetic acoustic emission signals, which is a novel method of the recognition of electromagnetic acoustic emission signals for the detection of metal cracks.

Conflicts of Interest

The authors declare no conflicts of interest regarding the publication of this paper.

References

[1] Pan, H. (2018) Development and Application of Lightweight High-Strength Metal Materials. *MATEC Web of Conferences*, **207**, Article No. 03010. https://doi.org/10.1051/matecconf/201820703010

[2] Ciampa, F., Mahmoodi, P., Pinto, F., *et al.* (2018) Recent Advances in Active Infrared Thermography for Non-Destructive Testing of Aerospace Components. *Sensors*, **18**, Article No. 609. https://doi.org/10.3390/s18020609

[3] Li, N., Wang, F. and Song, G. (2020) New Entropy-Based Vibro-Acoustic Modulation Method for Metal Fatigue Crack Detection: An Exploratory Study. *Measurement*, **150**, Article ID: 107075. https://doi.org/10.1016/j.measurement.2019.107075

[4] Marcantonio, V., Monarca, D., Colantoni, A., *et al.* (2019) Ultrasonic Waves for Materials Evaluation in Fatigue, Thermal and Corrosion Damage: A Review. *Mechanical Systems and Signal Processing*, **120**, 32-42. https://doi.org/10.1016/j.ymssp.2018.10.012

[5] Zheng, S., Vanderstelt, J., McDermid, J.R., *et al.* (2017) Non-Destructive Investigation of Aluminum Alloy Hemmed Joints Using Neutron Radiography and X-Ray Computed Tomography. *NDT & E International*, **91**, 32-35. https://doi.org/10.1016/j.ndteint.2017.06.004

[6] Ahmad, M.I.M., Arifin, A., Abdullah, S., *et al.* (2019) The Probabilistic Analysis of Fatigue Crack Effect Based on Magnetic Flux Leakage. *International Journal of Reliability and Safety*, **13**, 18-30. https://doi.org/10.1504/IJRS.2019.097011

[7] Dwivedi, S.K., Vishwakarma, M. and Soni, A. (2018) Advances and Researches on

Non Destructive Testing: A Review. *Materials Today*: *Proceedings*, **5**, 3690-3698. https://doi.org/10.1016/j.matpr.2017.11.620

[8] Xin, M.L., Chen, Y., Li, M.D., *et al.* (2018) The Research of Penetration Testing in the FRP Pipe Applications. *IOP Conference Series*: *Materials Science and Engineering*, **292**, Article ID: 012080. https://doi.org/10.1088/1757-899X/292/1/012080

[9] Roberts, T.M. and Talebzadeh, M. (2003) Acoustic Emission Monitoring of Fatigue Crack Propagation. *Journal of Constructional Steel Research*, **59**, 695-712. https://doi.org/10.1016/S0143-974X(02)00064-0

[10] Kumpati, R., Skarka, W. and Ontipuli, S.K. (2021) Current Trends in Integration of Nondestructive Testing Methods for Engineered Materials Testing. *Sensors*, **21**, Article No. 6175. https://doi.org/10.3390/s21186175

[11] Finkel, P. and Godinez, V. (2004) Electromagnetic Stimulation of the Ultrasonic Signal for Nondestructive Detection of Ferromagnetic Inclusions and Flaws. *IEEE Transactions on Magnetics*, **40**, 2179-2181. https://doi.org/10.1109/TMAG.2004.829313

[12] Zhang, C., Liu, S.Z., Yang, Q., *et al.* (2011) Design and Experiment of Electromagnetically Induced Acoustic Emission for Metal Crack Detection. *Advanced Materials Research*, **291**, 1278-1283. https://doi.org/10.4028/www.scientific.net/AMR.291-294.1278

[13] Jin, L., Liu, S., Zhang, C., *et al.* (2012) Amplitude Characteristics of Acoustic Emission Signals Induced by Electromagnetic Exciting. *IEEE Transactions on Magnetics*, **48**, 2953-2956. https://doi.org/10.1109/TMAG.2012.2196419

[14] Cai, Z. (2019) Study on the Orientation Detection of Surface Cracks by Electromagnetic Acoustic Emission. *International Journal of Distributed Sensor Networks*, **15**. https://doi.org/10.1177/1550147719843860

[15] Zhang, C., Liu, S.Z., Yang, Q., *et al.* (2012) Signal Recognition and Experiment for Electromagnetically Induced Acoustic Emission. *Transactions of China Electrotechnical Society*, **27**, 18-23.

[16] Sun, J., Xiao, Q., Wen, J., *et al.* (2016) Natural Gas Pipeline Leak Aperture Identification and Location Based on Local Mean Decomposition Analysis. *Measurement*, **79**, 147-157. https://doi.org/10.1016/j.measurement.2015.10.015

[17] Sun, Y. and Yu, J. (2022) Fault Feature Extraction of Rolling Bearings Using Local Mean Decomposition-Based Enhanced Sparse Coding Shrinkage. *Journal of King Saud University-Engineering Sciences*, **34**, 17-22. https://doi.org/10.1016/j.jksues.2021.11.011

[18] Zhang, Y., Liu, B., Ji, X., *et al.* (2017) Classification of EEG Signals Based on Autoregressive Model and Wavelet Packet Decomposition. *Neural Processing Letters*, **45**, 365-378. https://doi.org/10.1007/s11063-016-9530-1

[19] Towsyfyan, H., Gu, F., Ball, A.D., *et al.* (2019) Tribological Behaviour Diagnostic and Fault Detection of Mechanical Seals Based on Acoustic Emission Measurements. *Friction*, **7**, 572-586. https://doi.org/10.1007/s40544-018-0244-4

[20] Zhang, X., Xin, B., Zheng, Y., *et al.* (2020) Fiber Recognition with Machine Learning Methods by Fiber Tensile Fracture via Acoustic Emission Method. *Textile Research Journal*, **90**, 2552-2563. https://doi.org/10.1177/0040517520924130

[21] Li, Y. and Xu, F. (2021) Structural Condition Monitoring and Identification of Laser Cladding Metallic Panels Based on an Acoustic Emission Signal Feature Optimization Algorithm. *Structural Health Monitoring*, **20**, 1052-1073. https://doi.org/10.1177/1475921720945637

[22] Cavanaugh, J.E. and Neath, A.A. (2019) The Akaike Information Criterion: Background, Derivation, Properties, Application, Interpretation, and Refinements. *Wiley Interdisciplinary Reviews*: *Computational Statistics*, **11**, e1460. https://doi.org/10.1002/wics.1460